

## EVALUATION OF STRESS AND DISPLACEMENT IN HIP PROSTHESES WITH INCORPORATING HOLE AND FIN FEATURES USING FINITE ELEMENT METHOD

H. ABDULLAH<sup>1,\*</sup>, N. TALIB<sup>1</sup>, M. S. ZAKARIA<sup>2</sup>

<sup>1</sup>Department of Manufacturing Engineering,  
Faculty of Mechanical and Manufacturing Engineering,  
Universiti Tun Hussein Onn Malaysia, 86400 Parit Raja, Johor, Malaysia

<sup>2</sup>Fakulti Kejuruteraan Mekanikal, Universiti Teknikal Malaysia Melaka,  
Hang Tuah Jaya, Durian Tunggal, Melaka, Malaysia

\*Corresponding Author: haslinaa@uthm.edu.my

### Abstract

The typical distribution of stress in the femoral bone undergoes substantial changes following total hip arthroplasty (THA). With the introduction of a hip prosthesis, it bears a share of the load, resulting in reduced stress in certain areas of the bone and this will lead to stress shielding. Several factors influence stress shielding, including the geometry and cross-section of the hip prosthesis. Additionally, the displacement of the implant is also studied to identify the effects of additional features on displacement. This is because displacement measures the movements of the implant under physiological load. Therefore, in this study, three prostheses were constructed. The dimension of the prosthesis was based on the size of the patients' bone. Two of them had additional fin and hole features in the proximal part of the prosthesis. Finite element analysis was implemented to examine stress distribution under normal walking conditions. Based on simulations, it was found that the addition of features to the basic design increased stress values in the fin and hole regions at the proximal part of the prosthesis. Additions of fins and holes features have caused increments of stress of almost 170% and 85%, respectively as compared to conventional implant. However, for the displacement, it was found that the addition of holes features at the proximal area decreases the displacement by approximates 62%. As conclusion, this demonstrated that the cross-section and geometry of the prosthesis significantly affected stress and displacement distribution. At the same time, it showed that the finite element method could predict the performance of hip implants.

Keywords: Finite element method, Hip arthroplasty, Hip prosthesis, Stress distribution.

## 1. Introduction

Hip replacement or hip arthroplasty is a surgery employed to relieve hip pain and discomfort. It is a common orthopaedic surgery that replaces the hip joint and gives the body support. The femoral part consisting of the femoral head and ball head will be replaced by the implant and acetabular cup [1]. Osteoarthritis is the most prevalent disorder causing deterioration of the hip joint and can cause pain, stiffness, crepitus, instability, and weakness in the muscles [2]. Additional causes of hip joint injury include trauma, osteoarthritis, rheumatoid arthritis, bone tumours, and chronic pain, particularly in the elderly. The main issue with total hip replacement with a cementless type of implant is bone resorption surrounding the implant, which causes a body reaction between the implant and bone to cause the binding at the bone-prosthesis interface to dissolve [3]. One potential factor contributing to bone resorption is stress shielding, resulting from reduced in the load transmitted to the entire bone [4, 5]. If the implant absorbs a portion of the load upon insertion in the femoral canal, the transferred load to the cortical bone may alteration, leading to a decreased stress distribution between the implant and the bone surface.

When shielded from stress, the femur undergoes adaptive changes, including a metabolic reduction in mass through internal or external remodelling. This adaptation is reflected in increased bone porosity or thinning, corresponding to decreased load-bearing needs. Consequently, the bone may weaken, becoming more vulnerable to fragility. This mechanical compromise may possibly cause bone resorption, potentially causing implant loosening at the interface with the bone. Hence, it is essential during total hip surgery to uphold the preoperative load transfer to prevent resorption of the bone [6, 7]. Ongoing advancements in prosthesis development offer surgeons a broader range of options compared to the past, especially concerning structural integrity and biocompatibility.

Modifying the femoral stem's stiffness can enhance load transfer to its proximal end, consequently minimizing stress shielding. Various factors, for instance, type of materials, construction, and, cross-sectional implant influence the rigidity of the stem [8]. Joshi et al. [9] enhanced the implant model by incorporating a plate at the proximal, aiming to evenly spread the load across the whole femoral and alleviate the cause of excessive stress occurring in cortical bone. Furthermore, Chethan et al. [1] investigated the impacts of stem designs with circular, oval, ellipse, and trapezoidal shapes. Utilizing the Finite Element Method (FEM) for stress simulation under static loading, it was noted that all four hip implants demonstrated von Mises stresses below their yielding strength. Notably, trapezoidal and circular stems exhibited lower von Mises stress associated with oval and ellipse shapes. In addition, Chethan et al. [10] introduced the trapezoidal hip stem, exploring the encouragement of femoral head size on the stress dissemination. Additionally, Sahai et al. [11] suggested a lightweight design, incorporating a hip stem with a distal hole to analyse stress distribution.

Shorter stems offer benefits from transferring physiological loads from the proximal femur, potentially minimizing stress shielding [12, 13]. For the cementless step with the tapered wedge, in contrast to traditional mounted and fill up stems, occupies a smaller femoral bone region and achieves initial fixation by pressing into the proximal medullary cavity. Choosing for a short stem can be advantageous as it poses a smaller amount of invasiveness to the femoral bone marrow [13]. The prosthesis configuration plays a crucial role in stress shielding, influencing the contact dynamics at the interface of implant and bone. Numerous clinical experiments have highlighted the significance

of custom-fabricated implant designs, aiming to get an exact size at the proximal part of the trochanter section to decrease the stress distribution [14]. Stress shielding may be mitigated simultaneously by decreasing hip implant stiffness through the selection of materials with different properties. This can also be achieved through geometric modifications, such as reducing the stem length, including a collar at the neck of stem, or aligning the stem with the femoral canal, especially at the proximal. Additionally, a combination of these approaches has been explored [5, 15].

Besides stress shielding, stability also performs a significant role in ensuring the success of hip surgery. Mohammed et al. [16] performed a study to determine the influence of hip prosthesis design on the range of motion. Properly aligning the acetabulum and stem will enhance stability and maximize the range of motion. Meanwhile, Adebomojo [17] have been implementing topology optimization on the design parameters to obtain the best shape of the prosthesis to minimize stress and enhance stability. The weight of the prosthesis design and material also influences the total deformation and stability. Hence, Sahai et al. [11] designed a lightweight prosthesis based on a porous structure. Additionally, several holes were added to the distal part of the implant. The study results showed that the porous structure can improve the performance and success of hip surgery.

Despite the diverse array of materials, combinations, and geometries employed in implant development, there exists a finite lifespan for these implants, necessitating resurfacing. Consequently, there is a considerable opportunity for the advancement of new biomaterials and improved implant designs capable of surpassing the ten-year threshold [13, 14]. In the previous study by Abdullah et al. [18] the study focused on the effect of geometrical implant on the stability. Therefore, the main purpose of this research is to focus on the improvement of implants design by constructing a stem incorporating fin and groove characteristics for the analysis distribution of stress surrounded by the component of THR, which is stem and femoral bone. The inclusion of the additional features in the implants design, it is expected to enhance the stress distribution and improve the performance of implant.

## 2. Materials and Methods

A three-dimensional bone was constructed based on patient's condition in Malaysia. The femoral bone is a complex structure, making constructing an accurate three-dimensional model challenging. However, the use of a computer tomography (CT) dataset simplifies the construction of the femoral bone's 3D model. Additionally, for the porous structures like cancellous bone, were modelled as a solid part. As suggested by Ishak et al. [19], because of processing the complicated geometrical structure, several amendments were made to the three-dimensional bone, including smoothing the anterior, posterior, lateral, medial, and distal areas of the femoral parts. Figure 1 depicts the finalized part of the hip femur bone. The entire hip joint was created by using the left leg of a patient as a reference.

The hip stem reference was generated using 3D computer-aided design (CAD) software. The stem size was determined based on the constructed femoral bone. Meanwhile, the stem model was validated through static structural analysis by using Finite Element Analysis in Abaqus. Using the stem model design depicted in Fig. 2(a) as the baseline, two additional hip stem models with triangle holes and fin features were created, as explained in the Figs. 2(b) and 2(c) respectively. Although the three-dimensional bone model was constructed based on a single dataset, the

parameters for the hip implant, such as the neck-shaft angle and the diameter of the hip stem, still fell within the acceptable range [20]. Choosing materials is a crucial factor in the design process, considering performance and compatibility considerations. In this novel implant design, Ti-6Al-4V was selected as the material of preference, primarily due to its biocompatibility [21]. Table 1 contains information on the properties of both femur bone and the titanium alloy Ti6Al4V.

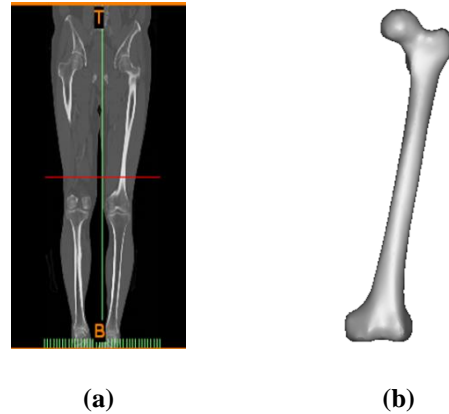


**Fig. 1. Construction three-dimensional femoral bone (a) 2D image of CT dataset (b) 3D model.**

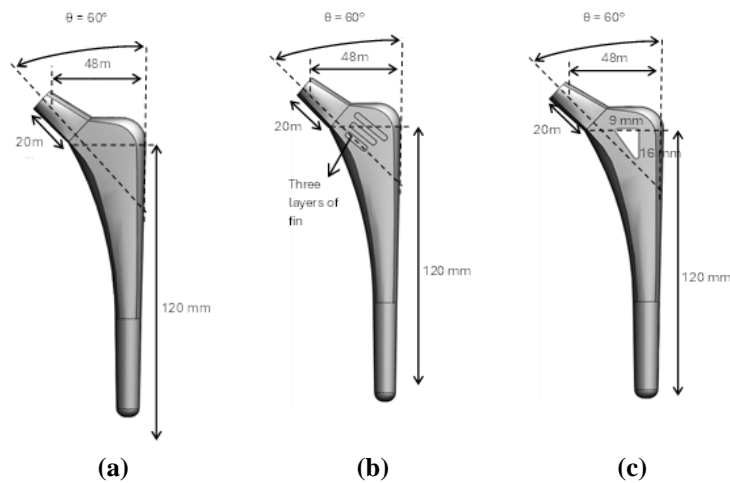


**Fig. 2. Hip prosthesis design (a) reference design (b) fin design (c) hole design.**

**Table 1. Properties of femoral bone and Ti6Al4V [22].**

Material	Tensile strength (MPa)	Elastic modulus (GPa)	Poisson's ratio ( $\nu$ )
Cortical bone	17.26	115	0.29
Ti6Al4V (prosthesis material)	110	485	0.3

This study utilized the Abaqus finite element software, chosen for its capability to perform contact analysis based on the type of tetrahedral meshing elements. Table 2 provides a summary of the total element count across all models. The number of elements was obtained based on the mesh study. The results of the mesh sensitivity study were shown in Fig. 3. The results indicated that mesh number 4 was well-converged, with a relative error of 3.70%. Although the error for the finer mesh number 5 is lower, an error of less than 5% was generally acceptable for most engineering studies and practical in terms of reducing computational cost.

The contact analysis at the bone-prosthesis interface has been conducted based on the analysis of contact elements. The whole implant-to-bone interface was modelled as absolutely bonded to indicate complete osseointegration of the implant body with the surrounding bone [19]. In this study, the master surface is referred to the prosthesis's area. Meanwhile, Fig. 4 shows the bone surface which is defined as the slave surface.

This study applied conditions simulating normal walking for loading and boundary conditions. The femoral bone underwent four distinct types of forces as depicted during typical walking conditions in Table 2. In addition, the hip joint positioned on Point 1 depended on the patient's weight. Point 2, which was the abductor muscle signified the total force applied by the gluteus muscle. This muscle helped the movement of rotation of the hip joint. Additionally, the tensor fascia lata at Point 2 contributed to abducting and flexing the thigh at the hip. The force values and locations were obtained from Duda et al. [21]. Figure 5 and Table 3 illustrate the force locations for normal walking conditions and the loading applied.

**Table 2. Elements used in simulation.**

Hip joint component	Number of elements	Total elements
Femoral bone	53903	59403
Reference design	5500	
Femur	46885	52522
Stem with hole	5637	
Femur	47944	55907
Stem with fin	7963	

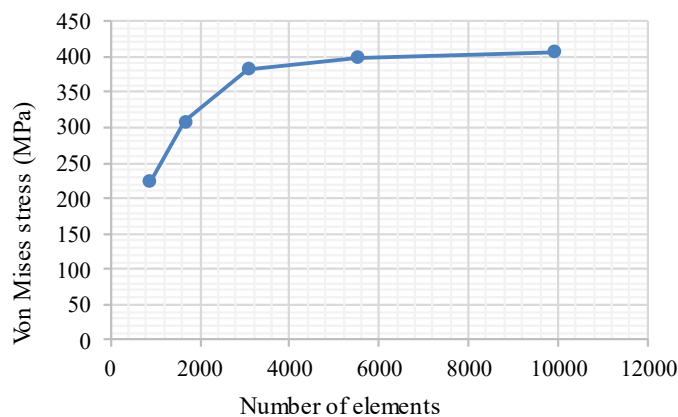


**Fig. 3. Results of mesh sensitivity study.**

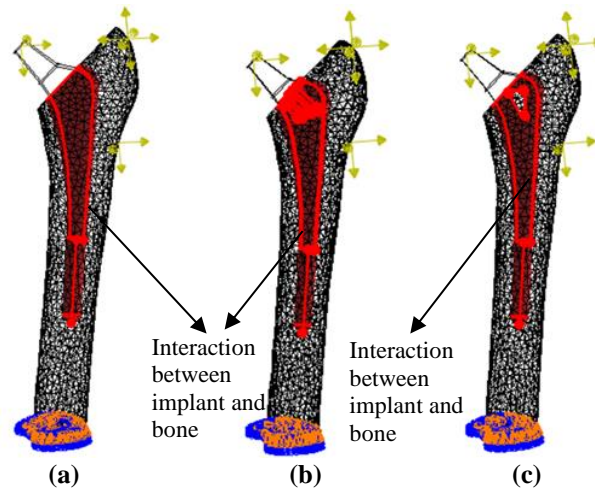


**Fig. 4. Interactions occur at the interface (a) reference design (b) hole prosthesis (c) fin prosthesis.**



**Fig. 5. Loading condition with boundary condition.**

**Table 3. Value of loading based on normal walking condition.**

Force Type (N)	X	Y	Z	Point
Joint contact load	433.8	263.8	-1841.3	1
Abductor force	-465.9	-34.5	695	2
Tensor fascia lata, distal part	-4	-5.6	-152.6	2
Tensor fascia lata, proximal part	57.8	93.2	106	2
Vastus lateralis	7.2	-148.6	-746.3	3

### 3. Results and Discussion

This study explains the prediction of stress shielding and stability to ensure the performance of additional features of fin and hole in the prosthesis

### 3.1. Effect of design of features on stress distribution

This simulation was conducted to study stress distribution within the hip prosthesis. This study applied full bonding to the surfaces between the hip prosthesis and the bone. Non-uniform stress distribution could reduce transmission of transferring load to the bone, leading to stress shielding and subsequent bone resorption. Figures 6, 7, and 8 show the stress distribution in the hip prosthesis based on normal walking condition. For all prosthesis, it illustrated that higher stress was produced at the proximal area of stem. This occurred due to by the removal of several parts at the section known as the trochanter to adapt the standard implant, while the load initiated by the muscle at trochanter persisted [9]. For the second design, which involved the addition of fin features in the proximal region, has resulted in a high stress value of 1076 MPa. This was attributed to the sharp features of the fins' edges that were generated. This indicated that the addition of fins to the prosthesis led to the generation of high stress.

Similarly, in the design with holes, despite Guo's [8] statement suggests that adding features such as holes and grooves could reduce the implant's weight and stiffness. Figure 6 demonstrates the generation of high stress in the area of the hole. This is due to the triangular shape and sharp edges of the created holes. Additions of fins and holes features have caused an increment of stress of almost 170% and 85%, respectively, as compared to conventional implant.

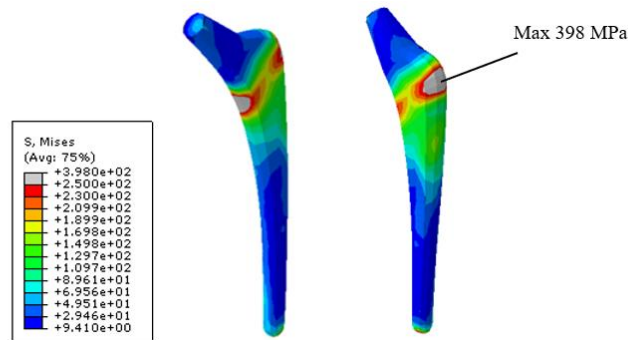


Fig. 6. Stress distribution at reference design.

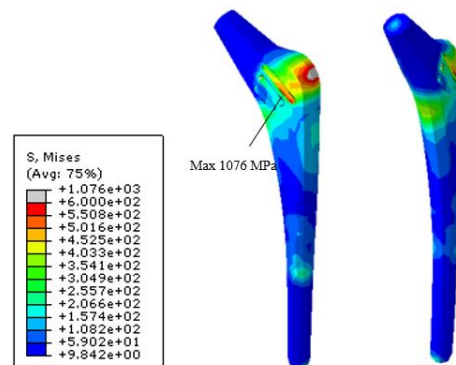
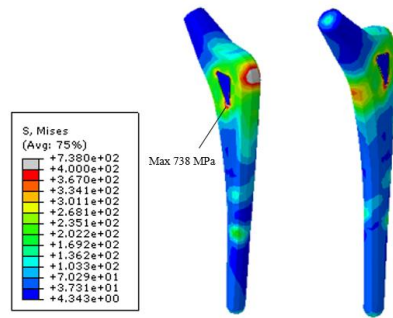


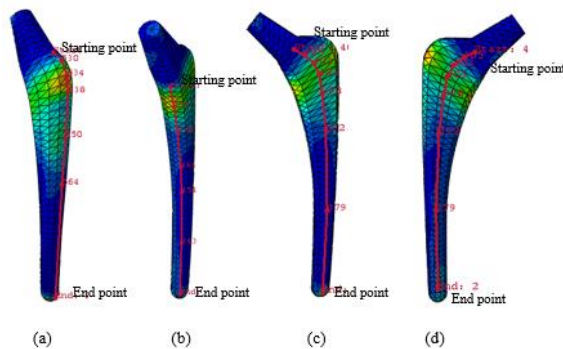
Fig. 7. Stress distribution at fin design.



**Fig. 8. Stress distribution in hole design.**

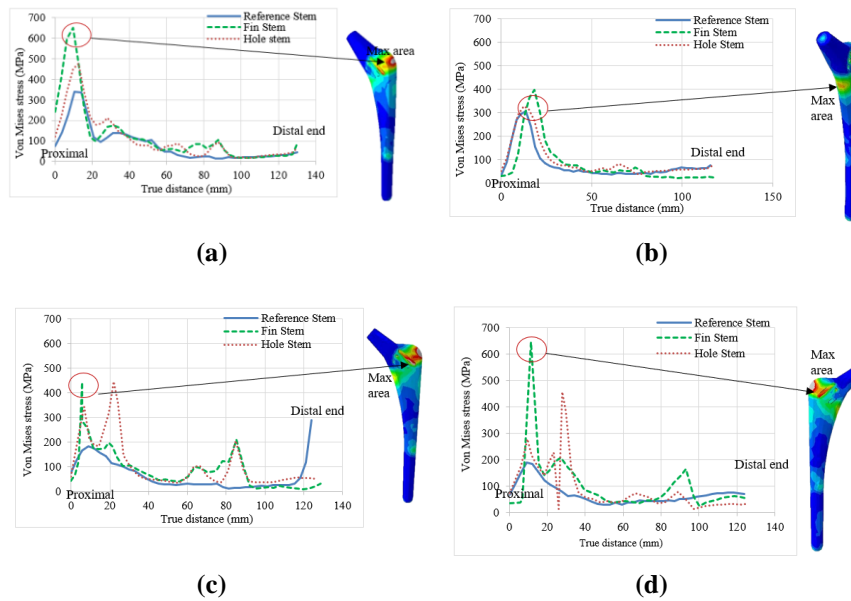
To plot a graph and measured the stress, a true path along lateral side, medial side, anterior side and posterior side has been selected as shown in Fig. 9. The comparison distribution of stress distribution along the lateral side, medial side, anterior and posterior was considered as suggested by Joshi et al. [9] and Jung and Kim [7].

Figure 10(a) indicates the stress distribution along the lateral side of the implant. It was found that additional features such as fins and holes increased the stress distribution at the proximal part of the implant. Similar results were obtained for the medial side as shown in Fig. 10(b). However, in contrast to anterior and posterior as illustrated in Figs. 10(c) and 10(d) respectively, the stress distribution fluctuates. Nevertheless, the highest stress values occurred in all design at the proximal part. The higher stress observed in this area resulted from the greater trochanter experiencing presumed loading from the muscle force or abductor. At the same time, amongst the overall stress comparisons for all sides, the reference design showed the lowest stress values followed by the hole and fin stem. The medial part, on the other hand, produced lower stress values as compared to the other sides of the prosthesis. The stress pattern was also almost the same for all designs, with high stress in the proximal part gradually decreasing towards the distal end of the prosthesis. The same distribution was obtained based on the FEM analysis conducted by Chen et al. [23]. This occurred due to bending caused by the forces applied at Point 1, Point 2, and Point 3 as stated in Table 2. On the contrary, Jung and Kim [7] observed a distinct stress distribution where is the greatest stress was localized at the tip of hip prosthesis. This variation can be attributed to differences in the applied loading conditions. In their study, only contact force was taken into consideration.



**Fig. 9. Node selection along (a) lateral side (b) medial side (c) anterior side (d) posterior side.**





**Fig. 10. Stress distribution along (a) lateral side (b) medial side (c) anterior side (d) posterior side.**

### 3.2. Effect from prosthesis features on displacement distribution

Figures 11, 12, and 13 illustrate the distribution of displacement on the reference prosthesis and prosthesis with additional features. It was found that the proximal region produced the highest displacement for all designs. This is because between the stem surface and bone. This relative displacement needed to be considered to identify the stability of an implant. If this relative displacement value exceeded the predetermined threshold which was  $40\text{ }\mu\text{m}$  -  $150\text{ }\mu\text{m}$ , it would lead to aseptic loosening and result in surgical failure [24]. In contrast to stress values, stems with holes were provided higher stability as compared to designs without features and designs with fins. This could be observed based on the graph of relative displacement occurring in the lateral, medial, anterior, and posterior regions. It indicated that the creating of holes in the implant or stem could enhance stability by assuming that bone growth occurred through the created holes. However, to ensure that no implant failure occurred due to holes, the design of the holes needed to be optimized to ensure that stress values in the regions were not high. Based on Fig. 9, stems with holes produced better stability for all regions, lateral, medial, anterior, and posterior. Additionally, the addition of features to the implant also helped to increase stability. Additionally, the addition of features to the implant also helped to increase stability.

Graph for displacement distribution was plotted to observe the effect of additional features in implant based on normal walking conditions. Figure 14(a) illustrates the displacement along the lateral side. The reference design showed the highest displacement, which might indicate it is less stable as compared to the other designs. This higher displacement could increase the risk of implant loosening, especially in the early stages of post-surgery. The fin stem showed a very similar

displacement pattern to the reference design but with a slightly lower displacement. In contrast to the hole stem, the figure observed a significant reduction in displacement, indicating better stability. Based on these results, the holes features might be reducing material density, leading to better load distribution. This design was also expected to encourage bone ingrowth, which enhanced stability over time. The same trend was observed for the medial side (Fig. 14(b)), anterior side (Fig. 14(c)), and posterior side (Fig. 14(d)), where the highest displacement occurred in the proximal part and gradually decreased towards the distal tip of the implant. This happened due to the principle of bending caused by forces acting on the joint and muscle in the abductor region [18].

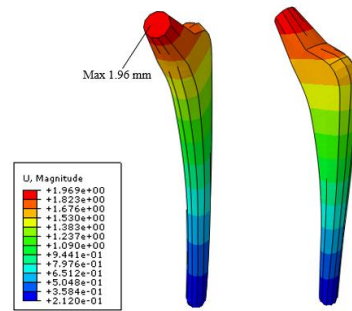


**Fig. 11. Displacement distribution on reference design.**

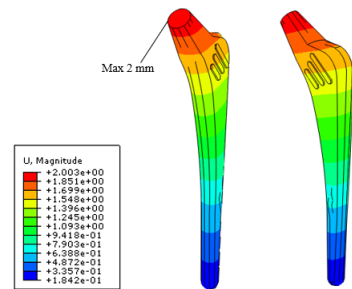


**Fig. 12. Displacement distribution on fin design.**

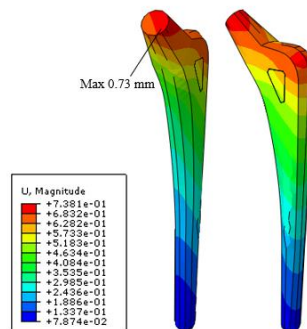


**Fig. 13. Displacement distribution on hole design.**

Additionally, for all paths, the reference design resulted in the highest displacement, followed by the fin design, while the hole stem provides better stability. Although the additional fins and holes on the stem led to higher stress, these features could provide good stability. Therefore, it is recommended that the implant design can be improved with consideration of rounded corners and fillets at the holes and fin's part. At the same time, surface treatments such as polishing, anodization, or coating with bioactive materials could reduce surface roughness and improve the fatigue resistance of the implant, thereby minimising wear and the risk of fractures [25]. At the same time, a comprehensive analysis should be conducted to balance the trade-offs between stress concentrations and displacement stability, ensuring that the design achieves optimal mechanical performance without compromising structural integrity.

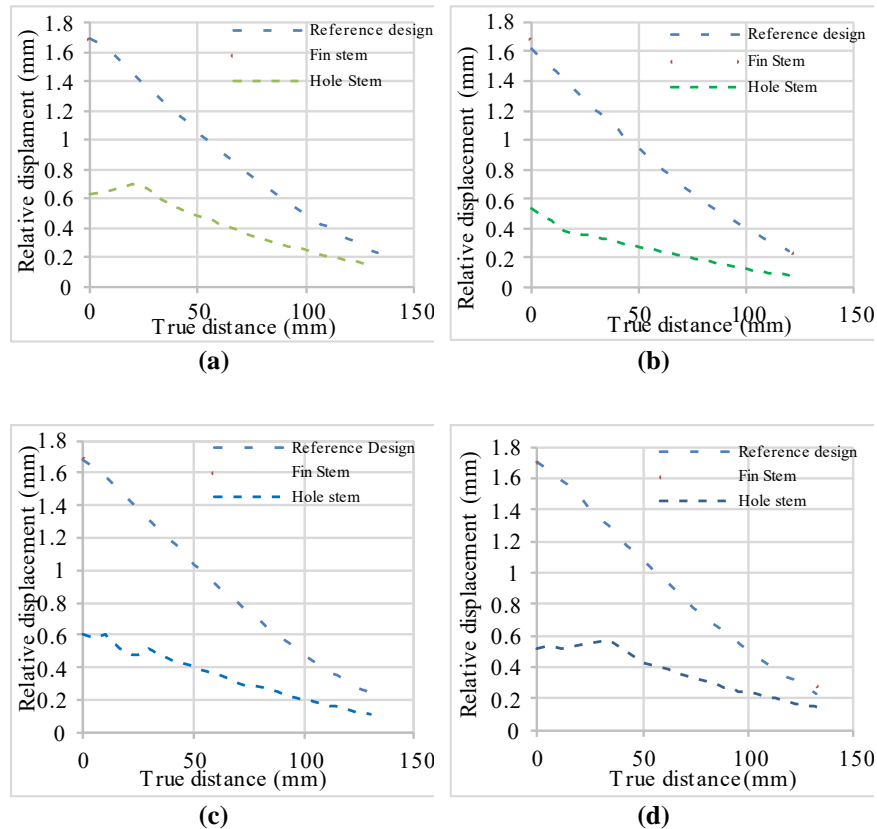


**Fig. 14. Displacement distribution (a) lateral side (b) medial side (c) anterior side (d) posterior side.**

#### 4. Conclusions

It is crucial to evaluate the stress and displacement distribution in the stem to improve and enhance the performance of hip prosthetics in hip replacement. This study uses finite element modelling to analyse the stress and displacement distributions in three different prosthesis designs with additional features such as layers of fin and hole at

the proximal part. Based on the simulation, adding features like fins and holes has increased the value of stress at the proximal are approximates 170% and 85%, respectively compared to conventional implant. This condition will lead to stress shielding and bone resorption since less load has been transferred to the bone. Therefore, it can be deduced that the geometry and cross-sectional characteristics significantly impact the stress distribution.

In contrast to displacement, additional feature of holes helps to decrease the displacement by around 62%. These findings reveal that while the addition of fins and holes in the prosthesis increases stress concentrations, it can also enhance stability and reduce displacement. These results highlight the importance of thoroughly balancing design features to optimise hip stem performance. Although this study provides valuable insights, it is limited by not considering the effect of bone growth and long-term effects. Future research should explore the biomechanical effect to understand implant design further and improve it.

### Acknowledgements

This research was supported by University Tun Hussein Onn Malaysia (UTHM) through Tier 1 (vot Q384).

### References

1. Chethan, K.N.; Bhat, S.N.; Zuber, M.; and Shenoy, S.B. (2019). Finite element analysis of different hip implant designs along with femur under static loading conditions. *Journal of Biomedical Physics and Engineering*, 9(5), 507-516.
2. Young, J.J.; Skou, S.T.; Koes, B.W.; Grønne, D.T.; and Roos, E.M. (2020). Proportion of patients with hip osteoarthritis in primary care identified by differing clinical criteria: A cross-sectional study of 4699 patients. *Osteoarthritis and Cartilage Open*, 2(4), 100111.
3. Agarwal, S. (2004). Osteolysis - Basic science, incidence and diagnosis. *Current Orthopaedics*, 18(3), 220-231.
4. Fukuoka, K.; and Todo, M. (2018). Analysis of principal stress projection in femur with total hip arthroplasty using CT-image based finite element method. *International Archives of Orthopedic Surgery*, 1(1), 1-10.
5. Naghavi, S.A. et al. (2023). A novel hybrid design and modelling of a customised graded Ti-6Al-4V porous hip implant to reduce stress-shielding: An experimental and numerical analysis. *Frontiers in Bioengineering and Biotechnology*, 11, 1092361.
6. Kuiper, J.H. (1993). *Numerical optimization of artificial hip joint designs*. Drukkerij Leijn, Netherlands.
7. Jung, J.M.; and Kim, C.S. (2014). Analysis of stress distribution around total hip stems custom-designed for the standardized Asian femur configuration. *Biotechnology and Biotechnological Equipment*, 28(3), 525-532.
8. Guo, L. et al. (2022). On the design evolution of hip implants: A review. *Materials & Design*, 216, 110552.
9. Joshi, M.G.; Advani, S.G.; Miller, F.; and Santare, M.H. (2000). Analysis of a femoral hip prosthesis designed to reduce stress shielding. *Journal of Biomechanics*, 33(12), 1655-1662.

10. Chethan, K.N.; Zuber, M.; Bhat, S.N.; and Shenoy, S.B. (2020). Optimized trapezoidal-shaped hip implant for total hip arthroplasty using finite element analysis. *Cogent Engineering*, 7(1), 1719575.
11. Sahai, N. et al. (2021). Designing & simulation of a lightweight hip implant stem: an FEM based approach. *Advances in Materials and Processing Technologies*, 8(3), 1126-1134.
12. Falez, F.; Casella, F.; Panegrossi, G., Favetti, F.; and Barresi, C. (2008). Perspectives on metaphyseal conservative stems. *Journal of Orthopaedics and Traumatology*, 9(1), 49-54.
13. Kaku, N.; Pramudita, J.A.; Yamamoto, K.; Hosoyama, T.; and Tsumura, H. (2022). Stress distributions of the short stem and the tapered wedge stem at different alignments: A finite element analysis study. *Journal of Orthopaedic Surgery and Research*, 17(1), 530.
14. Raffa, M.L.; Nguyen, V.H.; Hernigou, P.; Flouzat-Lachaniette, C.-H.; and Haiat, G. (2021). Stress shielding at the bone-implant interface: Influence of surface roughness and of the bone-implant contact ratio. *Journal of Orthopaedic Research*, 39(6), 1174-1183.
15. Liu, B.; Wang, H.; Zhang, N.; Zhang, M.; and Cheng, C.-K. (2021). Femoral stems with porous lattice structures: A review. *Frontiers in Bioengineering and Biotechnology*, 9, 772539.
16. Mohammed, W.; Abd-Elhaleem, M.; and Eltayeb, M. (2018). Design and simulation of hip prosthesis using finite elements methods to fulfill essential range of motion. *Proceedings of the International Conference on Computer, Control, Electrical, and Electronics Engineering (ICCCEEE)*, Khartoum, Sudan, 1-8.
17. Adebomojo, M. (2023). *Exploring finite element analysis and topology optimization for enhancing femoral prosthesis design*. PhD Thesis, Ulster University, Magee Campus, Londonderry.
18. Abdullah, H.; Zakaria, M.S.; and Talib N. (2024). Study of primary stability of hip implant for semi hip replacement by using finite element analysis. *Proceedings of the 2nd Human Engineering Symposium (HUMENS 2023)*, Pekan, Pahang, Malaysia, 133-144.
19. Ishak, M.I.; Daud, R.; Noor, S.N.F.M.; Khor, C.Y.; and Roslan, H. (2023). Influence of parafunctional loading conditions on the biomechanical behaviour of dental implant. *Journal of Engineering Science and Technology*, 18(2), 1237-1257.
20. Mandavgade, G.D.; and Deshmukh, T.R. (2018). Standardized hip implant by cluster analysis of anthropometry parameters of femur. *Journal of Medical Sciences*, 19(1), 11-16.
21. Duda, G.N.; Schneider, E.; and Chao, E.Y.S. (1997). Internal forces and moments in the femur during walking. *Journal of Biomechanics*, 30(9), 933-941.
22. Annanto, G.P. et al. (2018). Numerical Analysis of Stress Distribution on Artificial Hip Joint Due to Jump Activity. *Proceedings of the 3rd International Conference on Energy, Environmental and Information System (ICENIS 2018)*, Semarang, Indonesia, 73, 12005.

23. Chen, D.W.; Lee, M.S.; and Lin, C.-L. (2018). Finite element analysis of stresses from hip implants with different head sizes. *International Journal of Research Studies in Science, Engineering and Technology*, 5(5), 1-8.
24. Bieger, R.; Freitag, T.; Ignatius, A.; Reichel, H.; and Dürselen, L. (2016). Primary stability of a shoulderless Zweymüller hip stem: A comparative in vitro micromotion study. *Journal of Orthopaedic Surgery and Research*, 11, 1-6.
25. aliuk, V.I.; Vasilets, V.N.; Poliakov, A.M.; and Torkhov, N.A. (2022). Reducing the wear of the UHMWPE used in the total hip replacement after low-pressure plasma treatment. *Journal of Applied and Computational Pakh Mechanics*, 8(3), 1035-1042.